# SCIENTIFIC REPORTS

**OPEN**

There are amendments to this paper

# Neuronal firing rates diverge during REM and homogenize during non-REM

Hiroyuki Miyawaki[1,2], Brendon O. Watson[3] & Kamran Diba [1,4]

Neurons fire at highly variable intrinsic rates and recent evidence suggests that low- and high-firing rate neurons display different plasticity and dynamics. Furthermore, recent publications imply possibly differing rate-dependent effects in hippocampus versus neocortex, but those analyses were carried out separately and with potentially important differences. To more effectively synthesize these questions, we analyzed the firing rate dynamics of populations of neurons in both hippocampal CA1 and frontal cortex under one framework that avoids the pitfalls of previous analyses and accounts for regression to the mean (RTM). We observed several consistent effects across these regions. While rapid eye movement (REM) sleep was marked by decreased hippocampal firing and increased neocortical firing, in both regions firing rate distributions widened during REM due to differential changes in high- versus low-firing rate cells in parallel with increased interneuron activity. In contrast, upon non-REM (NREM) sleep, firing rate distributions narrowed while interneuron firing decreased. Interestingly, hippocampal interneuron activity closely followed the patterns observed in neocortical principal cells rather than the hippocampal principal cells, suggestive of long-range interactions. Following these undulations in variance, the net effect of sleep was a decrease in firing rates. These decreases were greater in lower-firing hippocampal neurons but also higher-firing frontal cortical neurons, suggestive of greater plasticity in these cell groups. Our results across two different regions, and with statistical corrections, indicate that the hippocampus and neocortex show a mixture of differences and similarities as they cycle between sleep states with a unifying characteristic of homogenization of firing during NREM and diversification during REM.

Firing rates vary among neurons and across time. The dynamic range of a neuron's firing is determined by a combination of membrane geometry, distribution and subtypes of ion channels, and synaptic efficacy[1–6]. Changes in these properties can potentially alter a neuron's gain function or "excitability", altering the neuron's encoding properties[7,8]. Recent evidence suggests that a neuron's firing rate is also homeostatically regulated[9–12], and that modifications in membranes and synapses can work to maintain the neuron's dynamic range[13,14]. Furthermore, a range of studies indicate that these modifications are at least partially state-dependent; the emerging picture is that firing rates of neurons increase during waking[10–12,15] and decrease during sleep[10–12,16], in a perpetual dance around a dynamic range.

The various waking and sleep states feature different activity levels of the neuromodulatory systems, which contribute uniquely to the excitability of neuronal circuits, network firing patterns, and the plasticity of their synapses[17,18]. For example, REM is characterized by high acetylcholine and low noradrenaline, serotonin and histamine levels, while waking and NREM respectively feature high and low levels of all these neuromodulators[17,18]. Unique brainstem and thalamocortical networks are also active within each state, producing state-specific oscillatory firing patterns[18–20]. The differing neuromodulatory and network backgrounds lead to different overall firing rates in REM, NREM, and waking[10–12], but averaging can also mask significant variations within each state[10,11,16].

It was recently shown that sleep yields a net decrease in the firing rates of both hippocampal[11] and frontal cortex neurons[10]. These changes were likely explained by synaptic downscaling[21], triggered in the hippocampus by

[1]Department of Psychology, University of Wisconsin-Milwaukee, P.O. Box 413, Milwaukee, WI, 53211, USA. [2]Department of Physiology, Graduate School of Medicine, Osaka City University, Asahimachi 1-4-3, Abeno-ku, Osaka, 545–8585, Japan. [3]Department of Psychiatry, University of Michigan Medical School, 109 Zina Pitcher Pl, Ann Arbor, MI, 48109, USA. [4]Department of Anesthesiology, University of Michigan Medical School, 1500 E Medical Center Drive, Ann Arbor, MI, 48109, USA. Correspondence and requests for materials should be addressed to K.D. (email: kdiba@umich.edu)

sharp-wave ripples and sleep spindles during NREM sleep[11], and incorporated over the course of REM sleep[11,16] and in the neocortex, triggered by alternating cycles of UP/DOWN states[22,23]. In Miyawaki and Diba[11] and Watson *et al.*[10], we took trouble to evaluate firing rate changes between different epochs of the same state (e.g. $NREM_i$ and $NREM_{i+1}$ epochs in sleep) to avoid confounds of state-dependent neuromodulation. However, some questions remain regarding how firing patterns of neurons of differing excitabilities change within each of these states and on transitions between these states, and how these compare between hippocampal and neocortical neurons. In particular, low and high firing neurons, with presumed low and high levels of excitability, are expected to be affected differently by activity-driven homeostasis and appear to bear differing levels of plasticity[2,9,24,25]. While this question was addressed to some extent in our previous work, understanding such effects is complicated by regression to the mean (RTM), for which the null hypothesis allows that firing rates of low-firing neurons should increase and those of high-firing neurons should decrease across any two comparative periods. A careful consideration of RTM is therefore necessary for a proper statistical evaluation of differential changes in low and high-firing cells.

In this report, we investigate changes in firing rates of neurons while accounting for RTM across both hippocampus and frontal cortex and both within and across transitions between different stages of sleep. We find that transitions to REM and NREM sleep states differentially affect low-firing and high-firing neurons in each state. In both hippocampus and frontal cortex, we find that REM sleep is marked by increased inhibition, and the spread between low- and high-firing neurons increases, while NREM results in a more homogenized and narrowed distribution of rates. These observations may help provide insights into the function and effects of sleep states on cortical networks of neurons.

## Results

### Differential effects of REM and NREM on higher- and lower-firing rate hippocampal neurons.

We previously recorded from populations of CA1 pyramidal cells and interneurons over multiple sleep and awake cycles[11]. Based on these data, we showed that mean firing rates in hippocampal pyramidal cells increased within NREM but decreased through transitions between NREM and REM, and such zig-zag change resulted in a net decrease across sleep[11,16]. However, it was not clear whether or not transitions between sleep states affect lower and higher firing pyramidal cells uniformly. To address this question, we sorted the pyramidal cells into five quintiles based on their rank-ordered firing rates (Fig. 1A) and investigated their changes within and across NREM and REM sleep epochs (Fig. 1B–G). Hereby, all analyses of neurons in these quintiles refer strictly to the pyramidal/principal cells, and interneurons are treated separately. To overcome potential confounds from RTM, here cells were sorted according to their firing rates over the entirety of the periods shown in each panel (see Methods for further details). Although all quintiles showed gradual firing increases within NREM and sudden decreases at the transitions to REM, the relative magnitudes of changes were different in lower- and higher-firing quintiles. Upon transitions to REM, lower firing cells showed large drops in activity, while higher firing cells showed little change ($\Delta$firing rate $= -41.5 \pm 3.3\%$, $-31.0 \pm 2.8\%$, $-14.6 \pm 2.9\%$, $-5.9 \pm 2.5\%$, and $11.4 \pm 1.9\%$ for low to high firing quintiles from last 1/3 of NREM to first 1/3 of REM, $F_{(4)} = 59.2$, $p = 1.1 \times 10^{-45}$, one-way ANOVA; Fig. 1B), effectively widening the distribution of firing rates and producing an increased coefficient of variation in the firing rates across neurons ($\Delta CV = 0.189 \pm 0.011$, $p = 1.0 \times 10^{-35}$, Wilcoxon signed-rank test; Fig. 1B,D). Interneuron firing increased at the transition to REM ($\Delta$firing rate $= 38.8 \pm 61.2\%$, $p = 1.1 \times 10^{-25}$, Wilcoxon signed-rank test), consistent with a more competition-driven network[26]. Within REM, firing rate changes were similar across quintiles and the CV did not change significantly (Fig. 1B,E,F). Upon the transition from REM to NREM, firing rates initially dropped in all quintiles. However, lower firing cells rebounded strongly (Fig. 1E) whereas higher firing cells were suppressed across NREM. Consequently, the CV of firing rates decreased (Fig. 1E,G, $\Delta CV = -0.155 \pm 0.014$, $p = 2.8 \times 10^{-21}$, Wilcoxon signed-rank test), indicating a narrowed and more uniform distribution of neuronal firing rates. This rebalancing of excitability within NREM was accompanied by decreased firing in interneurons. In summary, we observed differential dynamics in lower and higher firing neurons, with transitions to REM widening the distribution of firing rates and both transitions to and continuation of NREM narrowing the distribution of firing rates.

### Differential effects of REM and NREM on higher- and lower-firing rate neocortical neurons.

To examine whether similar state effects are also present in the neocortex, we extended these same analyses to neuronal spiking data recorded from frontal cortex of rats[10] and available on crcns.org (Fig. 2). Unlike in the hippocampus, firing rates increased at the transition from NREM to REM[12,27,28] (but also see refs[29,30]). However, similar to the hippocampus, firing rate distributions widened upon this transition, with higher-firing neocortical cells showing relatively larger increases at the transition to REM ($\Delta$firing rate $= 24.9 \pm 5.4\%$, $33.3 \pm 5.7\%$, $34.0 \pm 4.1\%$, $53.9 \pm 6.7\%$, and $41.3 \pm 3.8\%$, for each quintile from last 1/3 of NREM to first 1/3 of REM, $F_{(4)} = 4.3$, $p = 0.002$, one-way ANOVA; Fig. 2B), increasing the CV of firing rates ($\Delta CV = 0.033 \pm 0.021$, $p = 8.7 \times 10^{-5}$, Wilcoxon signed-rank test; Fig. 2B,F) alongside increased firing in interneurons ($\Delta$firing rate $= 15.1 \pm 48.7\%$, $p = 7.8 \times 10^{-4}$, Wilcoxon signed-rank test). Upon transitions from REM to NREM, firing rates decreased in the neocortex, and as in the hippocampus (Fig. 2E,G), the decrease was stronger in higher-firing than in lower-firing neurons. There was an accompanied decrease in interneuron firing and a significant decrease in the CV of firing rates across neurons ($\Delta CV = -0.034 \pm 0.021$, $p = 5.9 \times 10^{-4}$, Wilcoxon signed-rank test; Fig. 2E,G). The distribution of firing rates continued to narrow as NREM progressed (Fig. 2C). As the end of NREM approached, the firing rates began to increase, with further increases upon transition to REM. Overall, these results indicate that NREM and REM sleep states and the transitions between them have similar net effects on neurons with distributed firing rates in both the hippocampus and the neocortex.
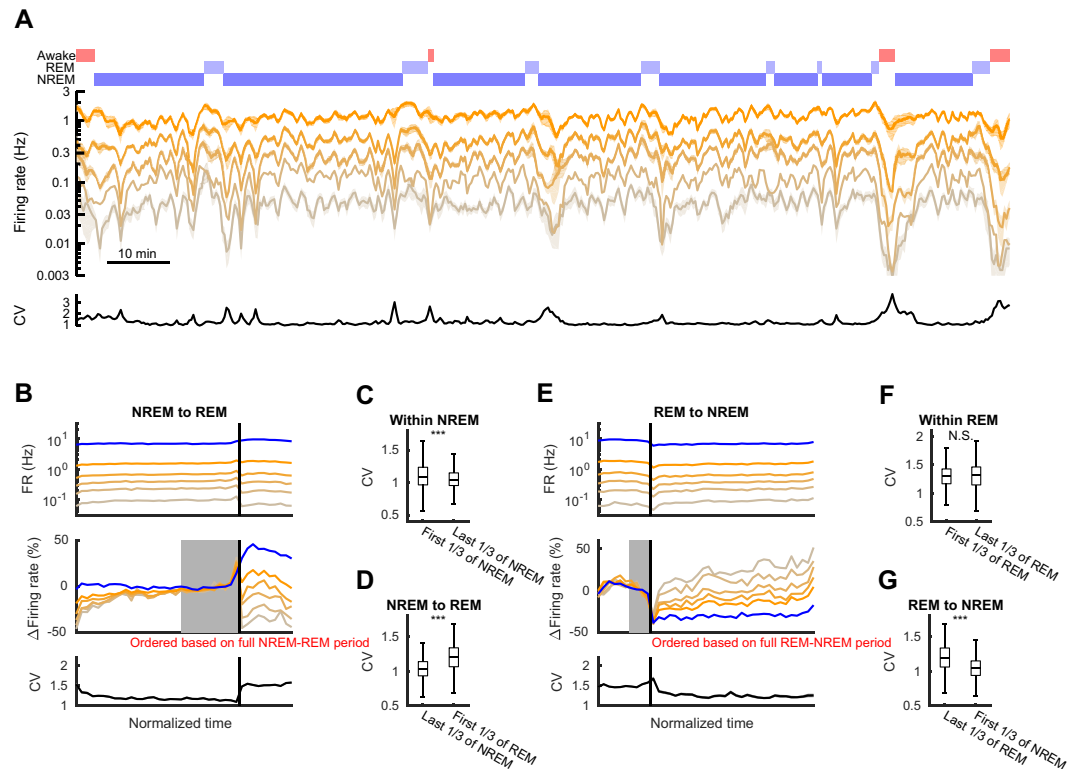
**Figure 1.** Firing rates of hippocampal neurons over transitions between sleep states. (**A**) An example period showing mean firing rates of hippocampal pyramidal cells (n = 94) sorted into five quintiles in sliding 1-min windows (20 s steps). The hypnogram and coefficient of variation (CV) are shown at top and the bottom, respectively. (**B**) Mean firing rates of each quintile of pyramidal cells (yellow lines) and interneurons (blue line) over transitions (vertical black line) from NREM to REM pooled across recordings (top panel). Quintiles were sorted independently for each analyzed NREM-REM doublet prior to averaging for presentation (see Table 1 for details). The middle panel shows the relative change from each quintile mean in the last third of the NREM epoch (the period indicated in gray). The bottom panel shows the mean CV of the complete distribution of pyramidal cells. (**C,D**) CV changes within NREM and on the transitions from NREM to REM. Significance was based on the Wilcoxon rank sum test. (**E–G**) Same with (**B–D**), but for transitions from REM to NREM. Alignment in E based on last third of REM (gray). Error bars and line shades indicate SEM. \*\*\*p < 0.001, N.S., not significant.

## Regression-to-the-mean and sorting effects on firing rate changes.

We wanted to better quantify these observations and to further evaluate how distributions of firing rates change within and across different sleep states. However, we first needed to better understand the relationship between variability and RTM in a population of neurons with log-normally distributed firing rates; ordering based on a part of analyzed data may bias the results due to RTM (Fig. 3A). We examined a simulated population of neurons where the source of variability is "multiplicative noise" proportional to each neuron's firing rate (Fig. 3B; see also Methods). Despite the absence of any change in our model population, lower-firing neurons show an apparent increased firing, while higher-firing neurons show an apparent decreased firing (Fig. 3C) when the quintiles are based on rank-ordering during the first epoch (i) of a sequence i-j. This is RTM and it can confound evaluations of true effects (e.g. from sleep). To control for RTM, we need to either rank-order cells by their mean firing rates over the entire sequence, as we did for analyses in Figs. 1,2, or else instate an appropriate correction. We introduced a shuffle correction in which we randomly flipped indices for epochs of the same state (e.g. $i$ and $k$ for a $NREM_i/REM_j/NREM_k$) and repeated the analysis multiple times to obtain a surrogate distribution for the change index of quintiles[11]. This surrogate data provided us with valuable "control" shuffle means and confidence intervals for each quintile. We defined the "deflection index (DI)" as the difference between the observed change index (CI) and the surrogate mean within each quintile. These DIs were not significantly different from zero when changes were due only to noise (Fig. 3C).

We then examined DIs under two scenarios with a simulated change in addition to noise: when firing rates increase across the population, either additively by a fixed amount for all cells (Scenario 1; Fig. 3D) or multiplicatively, by an amount proportional to each cell's initial firing rate (Scenario 2; Fig. 3E). The shuffle-corrected DIs effectively described and differentiated the two scenarios. Under Scenario 1 the additive increase produced a larger relative effect on the DI in low-firing cells than in high-firing cells (Fig. 3D), while under Scenario 2, the evaluated DI's correctly depicted a uniform increase across the population (Fig. 3E).

| States/transition type | Hippocampus | | Frontal cortex | |
| --- | --- | --- | --- | --- |
| | Pyramidal cells | Interneurons | Principal cells | Interneurons |
| NREM | 25717 cell-epochs in 462 epochs<br>25466 cell-epochs in 458 epochs | 3049 cell-epochs in 406 epochs<br>3045 cell-epochs in 405 epochs | 8097 cell-epochs in 232 epochs<br>7977 cell-epochs in 230 epochs | 785 cell-epochs in 205 epochs<br>735 cell-epochs in 203 epochs |
| REM | 15158 cell-epochs in 277 epochs<br>13106 cell-epochs in 244 epochs | 1783 cell-epochs in 241 epochs<br>1615 cell-epochs in 221 epochs | 3999 cell-epochs in 123 epochs<br>3463 cell-epochs in 109 epochs | 373 cell-epochs in 109 epochs<br>296 cell-epochs in 96 epochs |
| NREM-REM | 13159 cell-epochs in 240 transitions<br>11312 cell-epochs in 208 transitions | 1528 cell-epochs in 210 transitions<br>1334 cell-epochs in 188 transitions | 3380 cell-epochs in 105 transitions<br>2575 cell-epochs in 85 transitions | 319 cell-epochs in 93 transitions<br>222 cell-epochs in 76 transitions |
| REM-sNREM | 10355 cell-epochs in 190 transitions<br>8105 cell-epochs in 155 transitions | 1237 cell-epochs in 168 transitions<br>992 cell-epochs in 138 transitions | 3493 cell-epochs in 103 transitions<br>2995 cell-epochs in 87 transitions | 323 cell-epochs in 92 transitions<br>255 cell-epochs in 77 transitions |
| Wake-NREM | NA<br>4176 cell-epochs in 80 transitions | NA<br>724 cell-epochs in 100 transitions | NA<br>1697 cell-epochs in 48 transitions | NA<br>194 cell-epochs in 43 transitions |
| NREM-WAKE | NA<br>1014 cell-epochs in 29 transitions | NA<br>252 cell-epochs in 37 transitions | NA<br>408 cell-epochs in 28 transitions | NA<br>29 cell-epochs in 9 transitions |
| REM-WAKE | NA<br>298 cell-epochs in 20 transitions | NA<br>89 cell-epochs in 8 transitions | NA<br>60 cell-epochs in 28 transitions | NA<br>2 cell-epochs in 2 transitions |
| NREM-REM-NREM | 8767 cell-epochs in 165 triplets<br>6769 cell-epochs in 133 triplets | 1017 cell-epochs in 145 triplets<br>776 cell-epochs in 116 triplets | 2926 cell-epochs in 88 triplets<br>2123 cell-epochs in 66 triplets | 271 cell-epochs in 78 triplets<br>173 cell-epochs in 58 triplets |
| REM-NREM-REM | 5031 cell-epochs in 92 triplets<br>3257 cell-epochs in 60 triplets | 609 cell-epochs in 79 triplets<br>454 cell-epochs in 54 triplets | 1098 cell-epochs in 35 triplets<br>443 cell-epochs in 19 triplets | 98 cell-epochs in 31 triplets<br>41 cell-epochs in 19 triplets |
| SLEEP | NA<br>4983 cell-epochs in 88 sleeps | NA<br>585 cell-epochs in 74 sleeps | NA<br>1379 cell-epochs in 46 sleeps | NA<br>129 cell-epochs in 35 sleeps |
| WAKE-SLEEP-WAKE | NA<br>648 cell-epochs in 24 sequences | NA<br>304 cell-epochs in 37 sequences | NA<br>758 cell-epochs in 35 sequences | NA<br>71 cell-epochs in 21 sequences |

**Table 1.** Number of cells and states/transitions Numbers for time normalized analyses (Figs 1, 2 and 6A,B) and for *CI/DI* analyses (Figs 4, 5 and 6C–F) are shown in top and bottom of each cell. Since cells were counted multiple times for different epochs, we identify each instance used in analysis as a "cell-epoch".

**Firing-rate spread in REM and homogenization in NREM.** We next used the RTM correction methods described above to enable comparisons of firing rates in pairs of epochs. We did these analyses either within each state of sleep or across different stages of sleep. This approach is complementary to that shown in Figs. 1 and 2 and can serve as an independent verification of the observations shown there.

During NREM sleep, the average firing rates of hippocampal pyramidal neurons increased (mean $CI = 0.058 \pm 0.005$, $p = 5.9 \times 10^{-27}$, Wilcoxon signed-rank test). While the *CI* appeared to show the largest increase in low-firing cells, much of this apparent effect was due to RTM: in the shuffle corrected *DI*s, in fact the higher-firing quintiles showed the greatest relative increases (Fig. 4A, top row). In the frontal cortex the average *CI* decreased (mean $CI = -0.023 \pm 0.004$, $p = 3.2 \times 10^{-9}$, Wilcoxon signed-rank test). When cells were separated into quintiles, the *CI* appeared to indicate increased firing in lower-firing cells and decreased firing in higher-firing cells (Fig. 4A, bottom row), but those changes were also largely explained by RTM. After correction for RTM in the *DI*s, some increase was evident in the second lowest quintiles, along with a decrease in the two highest quintiles. Changes in firing rate distributions showed a consistent picture to the *DI* analyses (Fig. 4A, bottom) with the distribution for the hippocampus narrowing slightly and shifting towards increased firing, while that in the frontal cortex narrowing and shifting left towards decreased firing.

At the transitions from NREM to REM, hippocampal pyramidal cells decreased firing in all quintiles but the highest one, with the largest decrease in the lowest quintile ($DI = -0.213 \pm 0.019$, $-0.139 \pm 0.016$, $-0076 \pm 0.015$, $-0.038 \pm 0.011$, and $0.032 \pm 0.010$ for each quintile, all p values obtained by shuffling are $<0.001$; Fig. 4B, top row). Interneuron firing, on the other hand, increased ($CI = 0.142 \pm 0.013$, $p = 5.6 \times 10^{-22}$, Wilcoxon signed-rank test), indicating a new steady state in the balance between network excitation and inhibition (but see[31]). This increased inhibitory activity could potentially drive some of the decreased firing in pyramidal neurons[29] and allow for a winner-take-all mechanism whereby some high-firing cells dominate REM dynamics at the expense of lower-firing cells. These dynamics were somewhat different for the frontal cortex, however; at the onset of REM, principal neurons in the frontal cortex increased firing across quintiles, while interneurons showed little change ($DI = 0.094 \pm 0.029$, $0.187 \pm 0.023$, $0.181 \pm 0.019$, $0.188 \pm 0.020$ and $0.162 \pm 0.016$ for each quintile of principal neurons, p values $< 0.001$ relative to shuffles, $CI = 0.031 \pm 0.033$ for interneurons, $p = 0.03$, Wilcoxon signed-rank test). It is interesting to note however that the increased firing of hippocampal interneurons mirrored the overall increase in neocortical principal cell activity, consistent with neocortical control of hippocampal inhibition[32,33]. As a result of these changes, firing rate distributions became wider upon REM in both the hippocampus and the frontal cortex (Fig. 4B, right), consistent with our earlier analysis. Over the course of REM, we saw decreased firing across quintiles and interneurons in the hippocampus and in some quintiles of the neocortex (Fig. 4C). However, comparisons of the overall firing rate distributions did not reach statistical significance in the frontal cortex. The overall balance between excitation and inhibition therefore did not appear to change significantly within the course of REM states[34].

In contrast, when REM transitioned to NREM sleep, lower-firing quintiles showed increased firing while higher-firing quintiles and interneurons showed a firing decrease both in the hippocampus and in the frontal cortex (Fig. 4D). Interestingly, among the various dynamics we investigated only this transition from REM to NREM was marked by a renormalizing effect on firing rates across quintiles even after correction for RTM, and it was the only one we investigated that was marked by decreased firing of inhibitory cells in the hippocampus. NREM
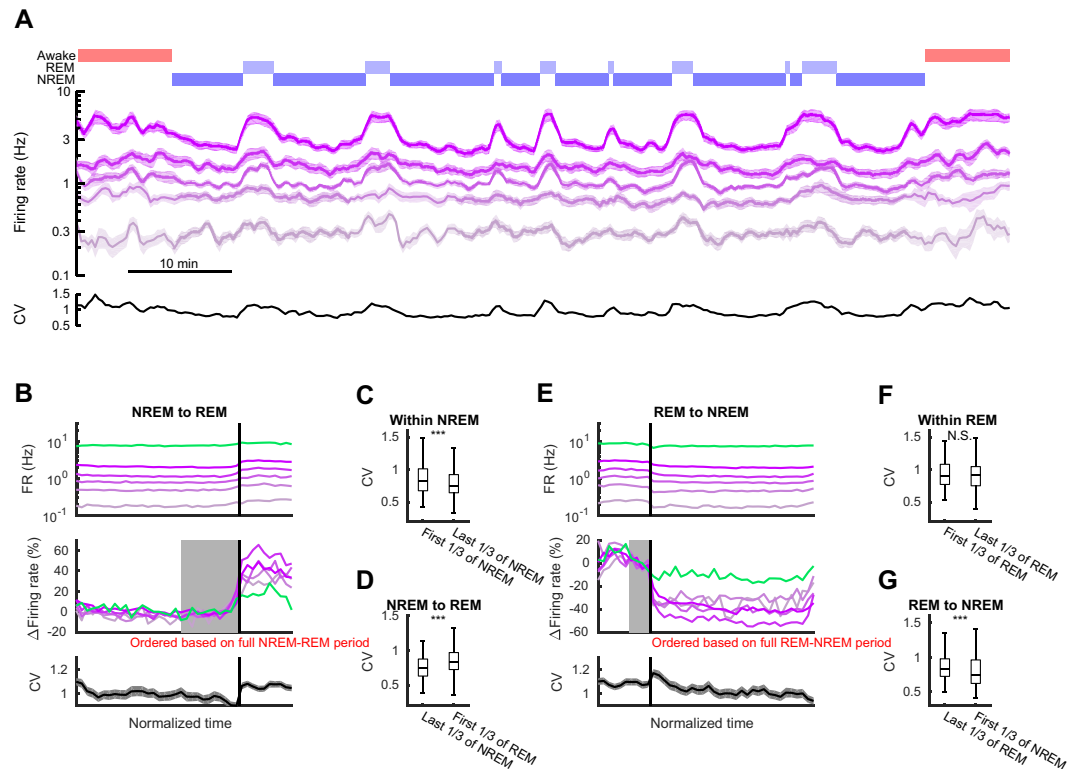
**Figure 2.** Firing rates of frontal neocortical neurons over transitions between sleep states. Same as in Fig. 1, but for frontal cortex. (**A**) An example period showing firing rates of frontal neocortical principal neurons (n = 89) in five quintiles (sliding 1-min windows with 20 s steps). Hypnogram and coefficient of variation (CV) shown at top and the bottom, respectively. (**B,E**) Firing rates of principal neurons (purple; top panels) and interneurons (green) over NREM-REM (**B**) and REM-NREM (**E**) transitions. Firing rates in the middle panels were normalized and aligned to mean in the last third of NREM in (**B**) and last third of REM in (**E**) (gray regions). CV of principal neuron firings on bottom panels. (**C,D,F,G**) CV changes within states and across sleep state transitions. Significance was based on the Wilcoxon rank sum test. Error bars and line shades indicate SEM. ***p < 0.001, N.S., not significant.

sleep therefore provided for the most uniform firing among the population of cells, potentially because of lower effective inhibition, whereas REM was marked by a widened distribution of firing activity.

**Neuronal firing changes at transitions to and from wake.** Our results thus far have outlined the effects of transitions and continuation of REM and NREM sleep states on neurons at different levels of excitability. We next applied these same methods to analyze the effects of transitions between sleep and waking on different quintiles and focused on our corrected DI analysis. Immediately upon transitions from waking to NREM sleep (direct transitions from wake to REM are rarely observed), the hippocampus showed increases in the middle of the distribution (Fig. 5A) whereas the frontal cortex showed a decrease in high-firing cells. Nevertheless, the wake-to-sleep transition was accompanied by decreased inhibition in the hippocampus ($CI = -0.076 \pm 0.016$, $p = 1.5 \times 10^{-6}$, Wilcoxon signed-rank test) but not in the frontal cortex ($-0.020 \pm 0.032$, $p = 0.60$, Wilcoxon signed-rank test) and a narrowing of the distribution of firing rates in both regions ($\Delta CV = -0.708 \pm 0.076$, $p = 2.4 \times 10^{-11}$, and $\Delta CV = -0.239 \pm 0.035$, $p = 6.1 \times 10^{-7}$ for the hippocampus and the frontal cortex, respectively, Wilcoxon signed-rank test). The distribution narrowing in the hippocampus again indicates a new steady state in the balance between excitation and inhibition, with increased activity in the three middle quintiles (Fig. 5A), whereas the frontal cortex narrowing was a result of decreased firing in the highest-firing quintile and a trend towards more increase in progressively lower firing cells.

In contrast, the distribution of firing rates widened at the onset of wake. At transitions from NREM to wake (Fig. 5B), hippocampal firing decreased significantly, particularly among the lowest firing quintiles. These changes resulted in a leftward shift in the firing rate distribution ($p = 2.9 \times 10^{-18}$, Kolmogorov-Smirnov test) and an increase in the CV ($\Delta CV = 0.915 \pm 0.137$, $p = 1.9 \times 10^{-7}$, Wilcoxon signed-rank test). In the neocortex, on the other hand, higher-firing principle neurons increased firing at the transitions from NREM to wake, essentially reversing the change from wake to NREM (Fig. 5A) and producing a significant increase in the CV of the distributions ($\Delta CV = 0.243 \pm 0.082$, $p = 0.019$, Wilcoxon signed-rank test). The transitions from REM to wake showed slightly different effects across quintiles (Fig. 5C). In sum, wake and sleep have contrasting effects on the activity of neurons in different quintiles, with sleep states displaying a more homogeneous distribution of firing rates and greater variation among the population during wake.
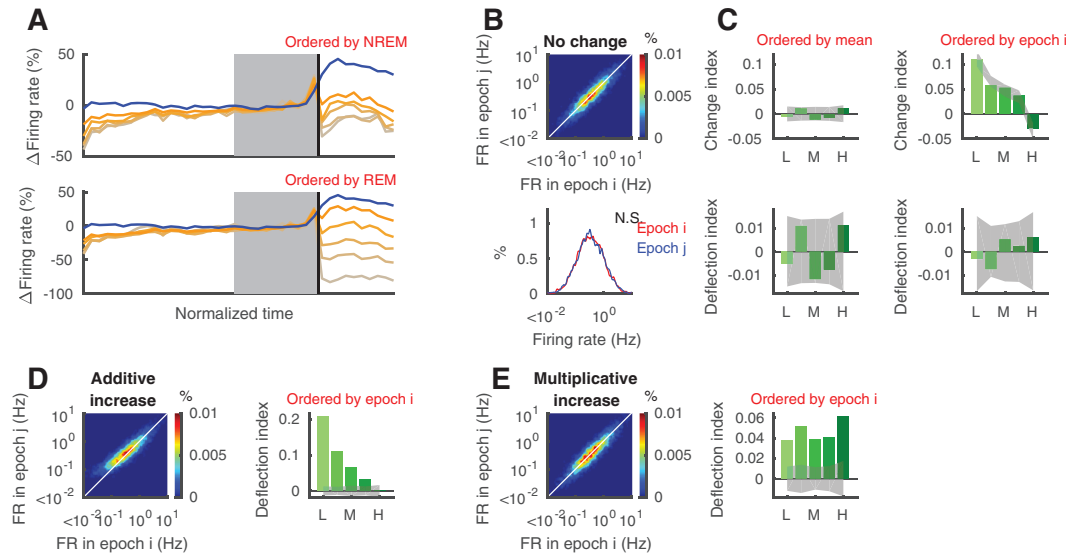
**Figure 3.** Deflection index can evaluate firing rate changes with correction for RTM. (**A**) Mean firing rates of hippocampal neurons in NREM-REM sequences as shown in Fig. 1B but different quintile separation (based on mean within NREM and REM for top and bottom, respectively). (**B**) Randomly generated firing rates with no change. (**C**) When cells are ordered based on the mean across combined states 1 and 2 (left column), there are no systematic difference on change index across quintiles. On the other hand, when cells are ordered based on state 1 alone (left column), systematic changes appear due to RTM. Deflection index (*DI*; for details see Material and Methods) can compensate for the effect of RTM (bottom panels). (**D,E**) In cases with non-zero changes in firing rate, *DI* is also significantly different from zero. Example of additive increase (**D**) and multiplicative increase (**E**). Gray bands indicate 95% confidence intervals obtained from shuffling (2000 times). Each example has 5000 cells whose firing rates are distributed log-normally.

## Lasting effects of sleep and sleep states on firing rate distributions.

These analyses describe a perpetually fluctuating pattern of neuronal activity across sleep and wake transitions, with alternating narrowing and widening of firing rate distributions. We next asked which of these effects persists across longer sleep sequences composed of multiple NREM and REM episodes. First, we analyzed state triplets composed of $NREM_i$-REM-$NREM_{i+1}$ or $REM_i$-NREM-$REM_{i+1}$ (Fig. 6A–D)[10,11,16]. Time normalized firing rates and CVs in the triplets further illustrated and confirmed the distribution narrowing and widening effects of NREM and REM epochs, respectively (Fig. 6A,B), in both brain regions. However, based on these plots it appeared that these distribution changes largely offset and cancelled one another. To better quantify these impressions, we again calculated *DI*s for quintiles in both regions and compared firing rate distributions and CVs. All hippocampal quintiles showed decreased firing between consecutive NREMs interleaved by REM (Fig. 6C; note also that these decreases were more uniform across quintiles than those reported in Miyawaki and Diba[11] because we have excluded epochs with >20% non-firing cells in the present analyses). Firing rate distributions were slightly but significantly shifted leftward ($p = 2.7 \times 10^{-5}$, Kolmogorov-Smirnov test), though CVs were not statistically significant ($\Delta CV = 0.024 \pm 0.009$, $p = 0.066$, Wilcoxon signed-rank test). In the frontal cortex, lasting effects of REM on $NREM_{i+1}$ versus $NREM_i$ were more subtle and lower in magnitude. Only *DI* of the lowest firing quintile was significantly decreased, and we did not detect differences in the firing rate distributions ($p = 0.99$, Kolmogorov-Smirnov test), or CVs ($\Delta CV = 0.004 \pm 0.011$, $p = 0.52$, Wilcoxon signed-rank test). In the $REM_i$-NREM-$REM_{i+1}$ triplets, significant changes were not detected in *DI*s, distributions, or CVs from either region.

Extending these analyses to the first and last NREM in continuous sleep (separated by longer sequences of alternating REM and NREM), we observed significant decreases across pyramidal cell quintiles in the hippocampus (Fig. 6E). In the frontal cortex, *DI*s were significantly negative only in the middle and highest firing quintiles. These indicate overall firing rate decreases resulting from sleep, consistent with previous reports[11,12,16]. Interestingly, the lowest firing quintile decreased most in the hippocampus while the highest firing quintiles decreased most in the frontal cortex. But while firing rate distributions were slightly shifted leftward in the hippocampus ($p = 6.1 \times 10^{-6}$, Kolmogorov-Smirnov test), the difference did not reach significance in the frontal cortex ($p = 0.22$, Kolmogorov-Smirnov test). Importantly, pairwise comparisons of the CVs did not detect significant changes in variability in either the hippocampus or the neocortex ($\Delta CV = 0.039 \pm 0.018$, $p = 0.093$ for hippocampus and $-0.010 \pm 0.019$, $p = 0.731$ for frontal cortex, Wilcoxon signed-rank test). These results therefore indicate that distribution changes through multiple sequential REM and NREM states, alternately dispersing and homogenizing firing rates, were counter-balanced throughout sleep in both the hippocampus and the neocortex, despite excitability decreases in both regions in both the population as a whole and in specific quintiles.

Lastly, we compared the last minute of wake before sleep to the first minute of wake following sleep (Fig. 6F). In the hippocampus, *DI*s were significantly negative across quintiles, with those for lower firing quintiles more negative than those for higher firing quintiles, and firing rate distributions and CVs were significantly different
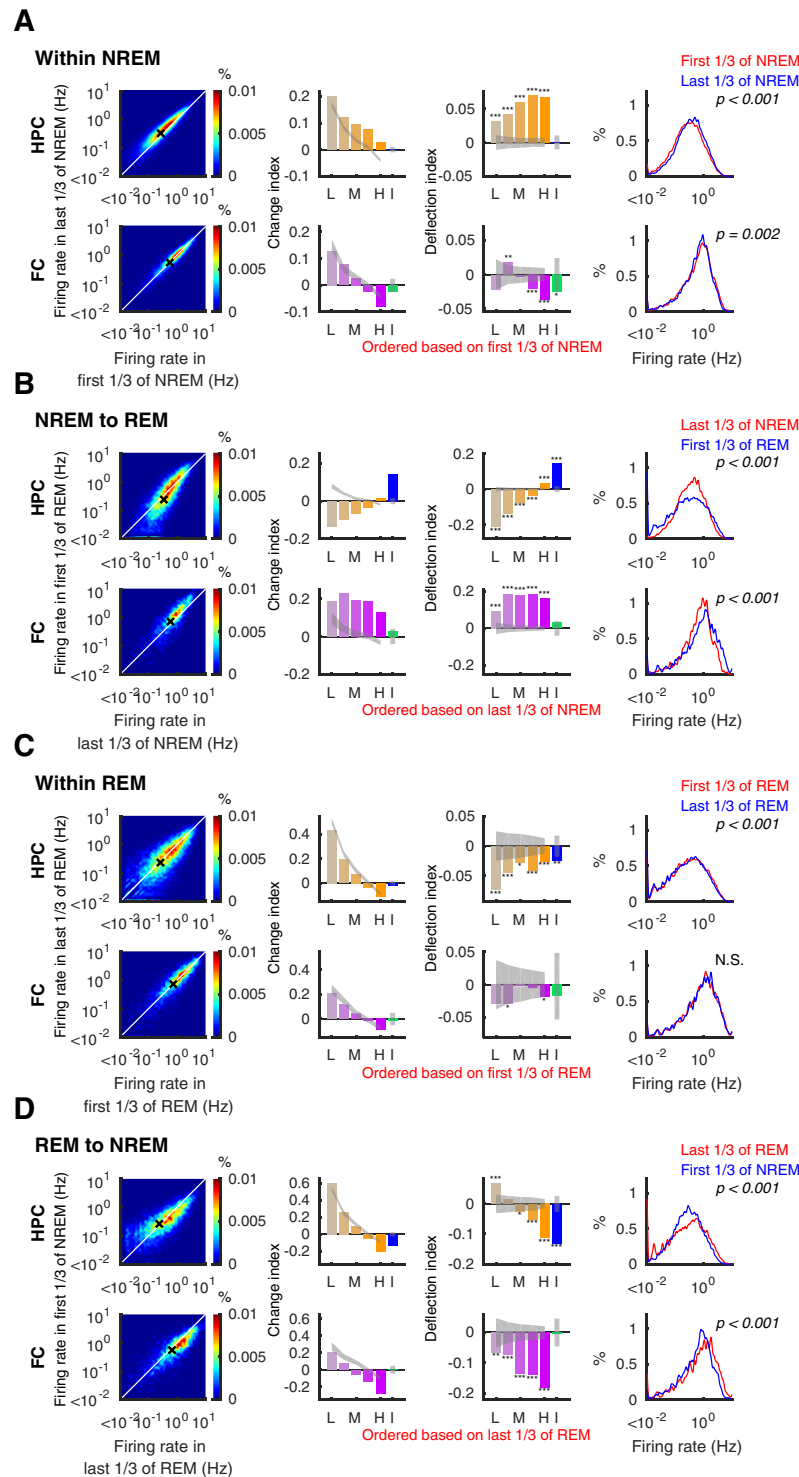
**Figure 4.** Firing rates diversify on transitions to REM and homogenize on transition to NREM. Firing rate changes within NREM (**A**), on transitions from NREM to REM (**B**), within REM (**C**), and on transitions from REM to NREM (**D**) in the hippocampus (HPC; top rows - orange) and the frontal cortex (FC; bottom rows - purple). Left panels show density (heat map) plots of firing rates. White lines indicate identity, and black crosses show means. Second and third panels illustrate change index (*CI*) and deflection index (*DI*) of each quintile of principal neurons (L: lowest quintile, M: middle quintile, H: highest quintile, yellow and purple bars) and interneurons (I, blue and green bars,) with 95% confidence interval (gray bands). Right panels show the firing rate distribution over all recorded principal neurons for the periods indicated in red and blue. P-values for the Kolmogorov-Smirnov test are indicated. $*p < 0.05$, $**p < 0.01$, $***p < 0.001$.

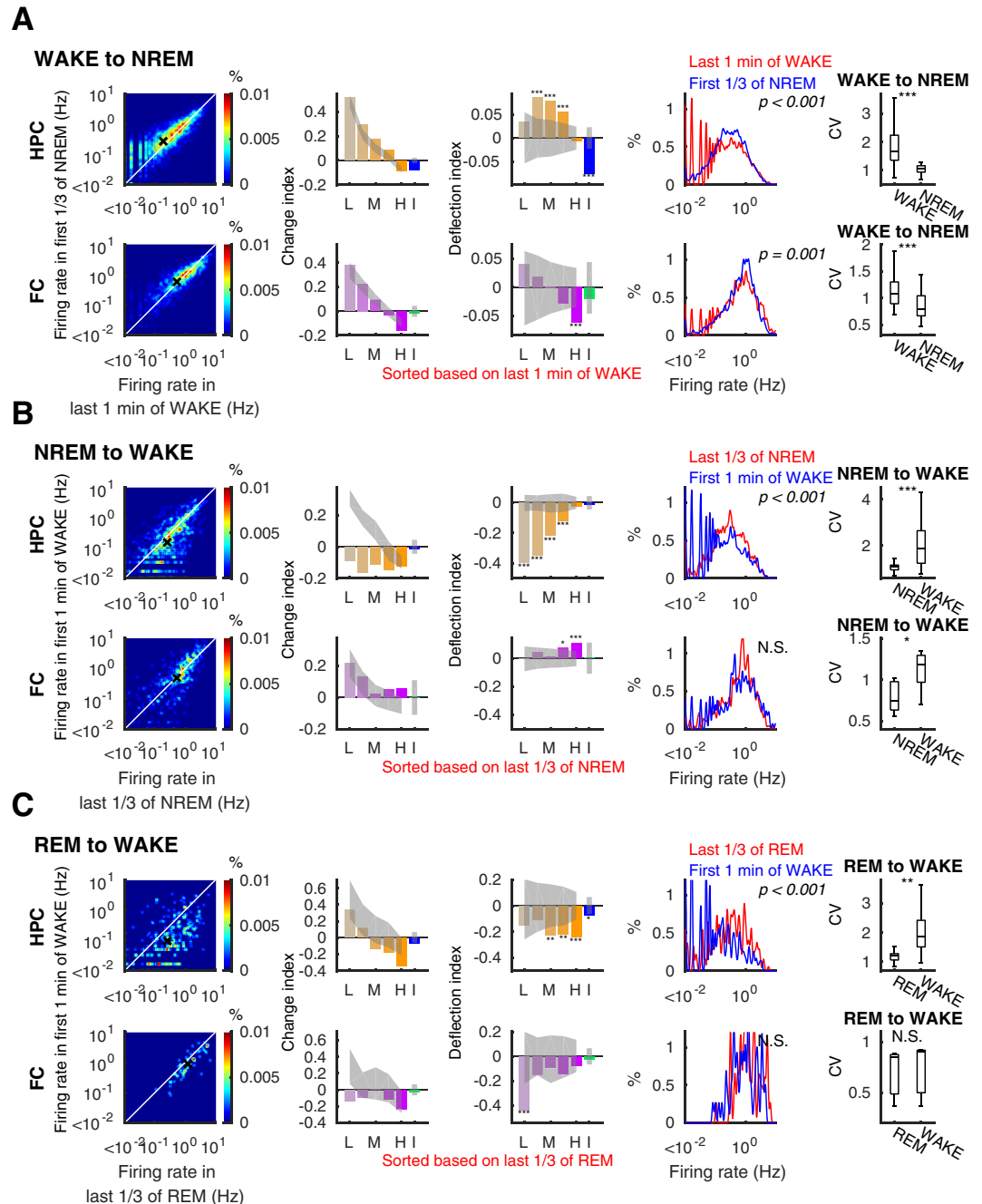**Figure 5.** Firing rate changes at transitions between wake and sleep. Similar to Fig. 4, firing rates (left panels), change (*CI*) and deflection (*DI*) indices (second and third panels) with 95% confidence intervals of shuffle mean (sheds on the bars), firing rate distribution (fourth panels) and coefficient of variation of firing rates (right panels) on transition from WAKE to NREM (**A**), NREM to WAKE (**B**), and REM to WAKE (**C**). Top and bottom rows in each panel present data from the hippocampus (HPC) and the frontal cortex (FC), respectively. L: lowest quintile, M: middle quintile, H: highest quintile, I: interneurons. P-values for Kolmogorov-Smirnov tests are indicated on the panels in the fourth column, *$p < 0.05$, **$p < 0.01$, ***$p < 0.001$.

(p = 0.007, Kolmogorov-Smirnov test, and $\Delta CV = 0.36 \pm 0.10$, p = $2.3 \times 10^{-4}$, Wilcoxon signed-rank test). On the other hand, principal neurons in the neocortex showed a significant increase in the lowest firing quintile and a significant decrease in the highest firing quintile, consistent with a narrowed distribution. However, neither firing rate distributions nor CVs were found to be significantly different across sleep (p = 0.97, Kolmogorov-Smirnov test, and $\Delta CV = -0.044 \pm 0.052$, p = 0.71, Wilcoxon signed-rank test). These results contradict our expectations based on previous analyses[10], which we will address in the Discussion section.
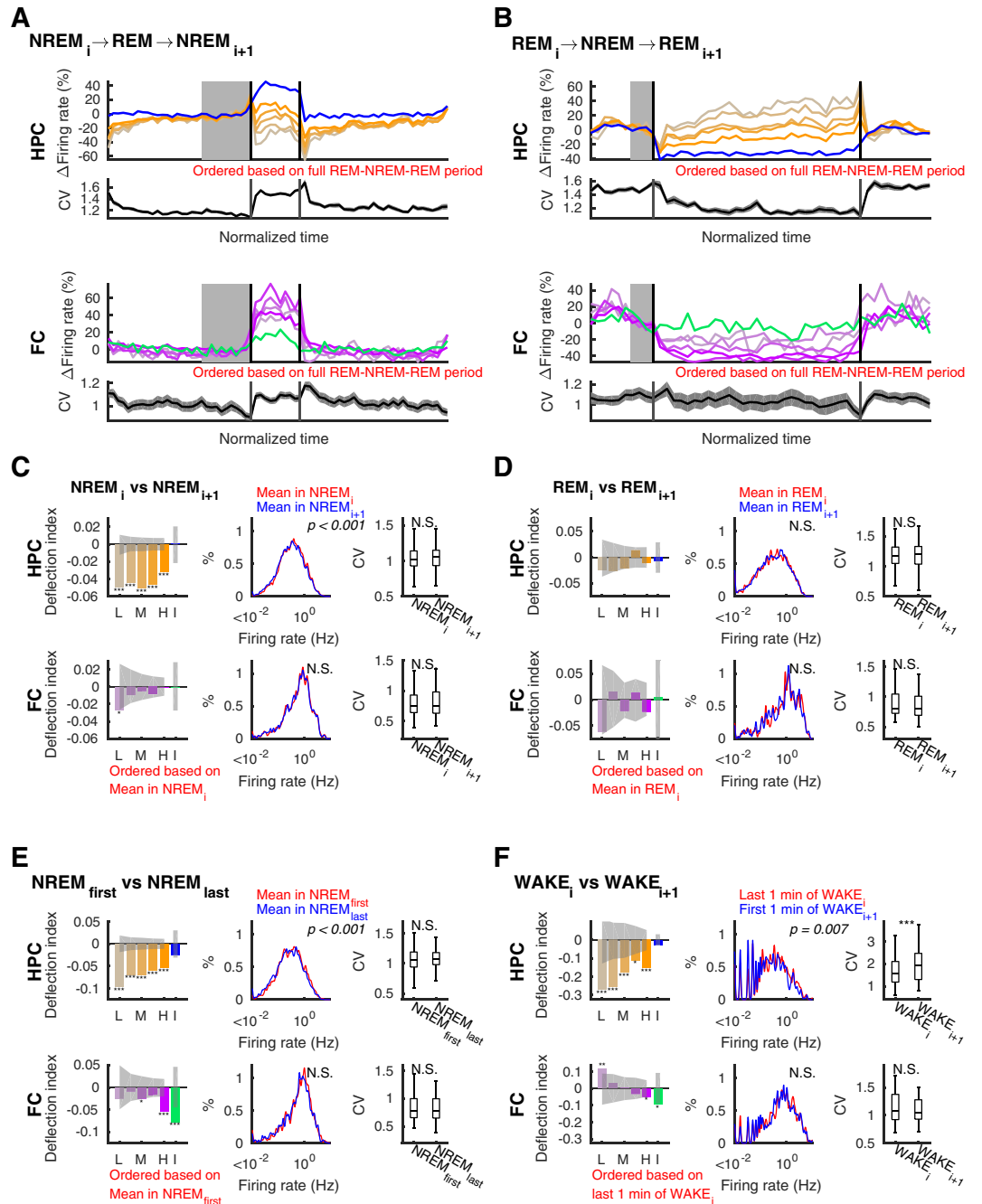
**Figure 6.** Net effects of sleep on neuronal firing distributions–analysis across state triplets. Effect of states as measured by net change from before to after that state. (**A**,**B**) Firing rates and coefficient of variation (CV) in the hippocampus (HPC; top panels) and in the frontal cortex (FC; bottom panels) in $NREM_i$-REM-$NREM_{i+1}$ triplets (**A**) and $REM_i$-NREM-$REM_{i+1}$ triplets (**B**) over time normalized for each epoch. Changes in firing rate of each quintile of pyramidal cells (orange shades) and interneurons (blue) in the hippocampus and frontal cortical principal neurons (purple shades) and interneurons (green) are relative to the mean of last third (shown in gray on the top panels and in blue on the bottom panels) of $NREM_i$ in (**A**) and last third of $REM_i$ in (**B**). (**C**–**F**) Deflection indices (*DI*), firing rate distributions, and CV of firing rates in (**C**) NREMs in NREM-REM-NREM triplets (**D**), REMs in REM-NREM-REM triplets, (**E**) between the first and last NREMs in each sleep, and (**F**) wake periods (last 1-min of $WAKE_i$ versus first 1 min of $WAKE_{i+1}$) separated by sleep in the hippocampus (top rows) and in the frontal cortex (bottom rows). L: lowest quintile, M: middle quintile, H: highest quintile, I: interneurons. P-values of Kolmogorov-Smirnov tests are indicated on the middle panels. Changes in CV were tested with the Wilcoxon rank sum test. Error bars and line sheds indicate SEM, sheds on bars indicate 95% confidence intervals of shuffle mean, *p < 0.05, **p < 0.01, ***p < 0.001, N.S., not significant.

### Effects of OFF states, LOW states, and microarousals on sleep-dependent firing changes.

Throughout NREM sleep, neurons throughout the brain undergo periods of suppressed firing of varying durations, each likely a result of a different mechanism[35–37]. DOWN/OFF states are a characteristic of the slow oscillations of NREM sleep, featuring hyperpolarized neurons and suppressed firing for approximately 50–100 ms. Neuronal activity during UP/ON states, exclusive of DOWN/OFF states, has been reported to resemble that of the awake brain[38]. Moreover, DOWN/OFF and UP/ON states appear to have differential effects on low versus high firing neurons[10]. Relatedly, LOW states and MAs are longer lasting periods of suppressed neuronal firing, likely related to brain-wide infraslow oscillations during periods of light sleep and/or brief awakening[35,36], which may also alter neuronal excitability in a subset of neurons[10,35,39]. We therefore examined the effects of removing these various substates of NREM sleep from the sleep/wake patterns we have so far examined. The most salient effect we observed was the obvious: that the exclusion of OFF states from NREM elevates firing rates, in both hippocampus and frontal cortex (Supplementary Fig S1–S5). Interestingly, in contrast to during intact NREM (Fig. 2B,E and Fig. 4A), neocortical firing rates increased across quintiles within NREM exclusive of OFF states (Supplementary Fig S2A,B, Supplementary Fig S3A), similar to the hippocampus. Importantly, the homogenization of firing rates within NREM was still seen in both the hippocampus (Supplementary Fig S1) and the neocortex (Supplementary Fig S2A-B and Supplementary Fig S3A,E). The exclusion of LOW and MAs also did not result in any notable differences (Supplementary Fig S1-S5), except that the effect of decreased firing over sleep was weaker, though still significant (Supplementary Fig S5D,F), as noted in a previous publication[35].

## Discussion

In this work, we aimed to provide a statistically controlled and analytically unified cross-regional examination of how the firing of populations of neurons is affected by sleep state cycling, to arrive at a better understanding of the function(s) of sleep states in mammals. Since many of our analyses depended on rank-ordering of firing rates and because low-firing and high-firing neurons regress to the mean by chance alone, in this study we designed our analyses to either prevent or correct for this effect. We used two methods; either we based the ordering on the mean firing rates over the entire period being considered, or else we measured all changes relative to a surrogate distribution obtained by random shuffles of the real data. These steps were necessary because ordering in any selected period produces illusionary normalization in a complementary period and any real changes must be evaluated in contrast to these non-negligible RTM effects. We found that, in general, sleep states and state transitions do not affect neurons uniformly, but that the changes depend on both the brain region and the relative activity of cells, which likely reflect a combination of neuromodulation of membrane excitability[40,41] and sleep-dependent network dynamics involving excitatory and inhibitory synaptic inputs to neurons[29,34,42–44].

Among the different state dynamics we investigated, NREM sleep was notable in homogenizing excitability across neurons. The transition from REM to NREM produced a greater relative decrease in high-firing cells in both hippocampus and neocortex, with an increase activity of low-firing cells in the hippocampus and a relatively smaller decrease in the neocortex. These changes at the onset of NREM serve to partially homogenize firing across both populations. In the frontal cortex, normalization continued during the NREM episode, and in both regions the coefficient of variation decreased at the onset and further throughout NREM. The onset of NREM was also marked by decreased firing in interneurons in the hippocampus, indicating a shift in the excitation/inhibition balance (see also[44]). These dynamics across two states, characterized by a major shift in cholinergic tone, are consistent with the greater relative effect of muscarine on several classes of inhibitory cortical interneurons[45]. Interestingly, atropine, a muscarinic acetylcholine antagonist, also produces increased bursting in hippocampal CA1 pyramidal neurons of lower excitability ("regular spiking") but decreased bursting in higher excitability ("bursting") cells[41]. This suggests that the decreased levels of neuromodulators along with the release from active inhibition allow for a rebalancing of pyramidal cell excitability during NREM sleep.

In contrast, the NREM to REM transition led to greater interneuron spiking and a greater separation of firing between low-firing and high-firing cells, increasing the CV in both regions. These winner-take-all type changes may be implemented in a recurrently connected circuit endowed with inhibition[46–48], such as region CA3, one synapse upstream from our CA1 recordings, or in layer 4 of the neocortex. The shift towards further competition may be supported by increased cholinergic levels during REM sleep that favor feedforward connections, such as from entorhinal cortex to region CA1[49,50], while neuromodulatory tone in NREM instead favors recurrently-generated activity[51]. It is also worth noting that hippocampal interneuron firing patterns across different sleep states closely mirrored those of cortical principal neurons (e.g. see Fig. 6A,B), consistent with neocortical control of hippocampal inhibition[32]. We also noticed that principal neurons showed relatively dramatic changes (e.g. see Fig. 6A,B) at the transitions between NREM and REM. These transition points may have unique properties: the transitionary period from NREM to REM sleep may in fact be a unique period of "intermediate sleep" that is inundated with both thalamacortical sleep spindles and theta oscillations[10,52], while the transitions from REM to NREM are often followed by LOW states and microarousals[35].

The net effects of these state transitions, from the first to the last NREM epochs during extended sleep sequences were mostly consistent with our previous reports[10,11], with some notable differences. Here, we find that distribution of the firing rates spread during REM and the homogenization during NREM largely cancel out in both hippocampus and neocortex, yielding a net effect of decreased firing rates in both regions over sleep[53]. These decreases were seen across all hippocampal quintiles over sleep, but preferentially in lower-firing neurons[11]. In the neocortex, decreases were less pronounced and were specific to high-firing cells, whereas Watson et al.[10] reported an additional parallel increase in firing of lower-firing neurons. This discrepancy between the present study and Watson et al.[10] may arise because of two factors: 1) Watson et al.[10] did not shuffle correct for RTM as in the current DI analysis and 2) Watson et al.[10] did not compare changes across entire episodes of NREM sleep, but rather across bouts or "packets" of NREM. The first and last packets of NREM fall onto the first and last thirds of NREM, and indeed, we observed a narrowing of frontal cortex firing rate distributions within each NREM episode over this period (see

Fig. 4A). It should also be noted that the comparison of $WAKE_i$ versus $WAKE_{i+1}$ (Fig. 6F) showed simultaneous firing increases in low-firing cells and firing decreases in high-firing cells, consistent with Watson et al.[10].

We and others have conjectured that the slower firing rate decreases over sleep, on the other hand, are produced by the downscaling of synaptic connections[11,12,16,21]. Network modeling also supports the notion of a strong link between the strength a neuron's connectivity and its firing rate[2,54]. Hippocampal changes across sleep (Fig. 6E,F) are consistent with an additive change (e.g. Fig. 3C), which indicates hippocampal firing decreased by a similar amount across cells. If the conjecture between synaptic connection and firing rate is correct, the uniform decrease of firing rates could imply a uniform weakening of synaptic connections which effectively improves signal-to-noise in higher-firing cells[21] (see also[53]). A recent study employing scanning electron microscopy of synaptic connections in the cortex supports this analysis; following sleep but not waking, smaller axonal-spine interfaces were observed in the four lower quintiles, with a lesser or no effect in the highest quintile[55]. Higher-firing neurons appear to show the least plasticity, perhaps as a consequence of rigidity or saturated synapses[24]. These distinctions may also reflect differences in neuronal subtypes within the CA1 pyramidal layer[50,56] that exist throughout the cortex[57], though surprisingly in the frontal cortex we saw the greatest decrease in firing across sleep in the higher-firing quintile (but see discussion points below).

While these observations demonstrate a remarkable degree of agreement about the effects of wake and sleep states on neuronal firing in the hippocampus and the frontal neocortex, some inter-regional differences were also evident in the responses of quintiles. All quintiles in hippocampus showed a prominent firing rate decrease from the beginning of sleep to the end (measured either from first to last NREM or from prior WAKE to subsequent WAKE), while in frontal cortex the net effect of sleep was more differentiated, with firing-rate decreases specific to the highest-firing quintile. Other notable intra-sleep differences between hippocampus and frontal cortex were found during the course of NREM episodes and at the transition from NREM to REM. A possible source of differences in hippocampal versus cortical profiles is that the cortex has DOWN/OFF states—periods of temporary network silence during NREM—which are not as clearly defined in the hippocampus[37,58]. The predominance of DOWN/OFF states can potentially account for the relatively decreased firing activity in the neocortex during NREM (see also[12]), particularly in the highest firing rate groups as slow waves in NREM develop, and the strong rebound in firing in these quintiles at the onset of REM sleep. Nevertheless, when we excluded OFF periods from our analysis, both hippocampal and frontal cortical neurons showed similar homogenization as before. On the other hand, LOW states and microarousals at the onset of NREM seem to have stronger suppressive effects on the firing of hippocampal neurons[35]. These apparent inter-regional differences may also arise because recordings and unit and state detection were performed by different experimenters in different labs. It is worth noting that overall firing rates were higher for the frontal cortex recordings than for the hippocampus recordings, so that lowest quintiles in the frontal cortex fire at similar rates to the middle quintiles in the hippocampus. Hence, sleep states may have effects that depend on absolute rather than relative firing rates and the normalizing and dispersing effects of NREM and REM sleep, respectively, represent broad effects of the neuromodulatory tones under different brain states.

In summary, our study provides a unified comparison of the effects of sleep and wake states on large populations of frontal cortical neurons and hippocampal neurons and highlights the importance of controlling for regression to the mean. Overall similarities and some specific differences were revealed - with commonalities including alternating patterns of firing rate homogenization and diversification in NREM and REM sleep, respectively, against a background of decreasing firing rates over the course of sleep. Progress in this line of inquiry will help us better understand the specific roles of different brain states in the function and homeostatic maintenance of neuronal circuits.

## Methods

We re-analyzed data previously recorded from hippocampal CA1 region of four male Long Evans rats[11,35] and frontal cortex of 11 male Long Evans rats[10]. Units were separated into putative pyramidal and principal cells and putative neurons based on spike waveform, the histogram of inter-spike-interval distribution, and mean firing rate[10,59,60]. In total, we recorded and analyzed 1017 putative pyramidal cells and 116 putative interneurons from the hippocampus and 995 putative principal cells and 126 putative interneurons from the frontal cortex. We analyzed these cell groups separately and, unless otherwise specified, by high and low-firing neurons we refer strictly to those units from the putative pyramidal/principal cell population. Details of the experimental protocols, including animals, surgery, electrophysiological recording, spike detection and clustering, and sleep detection can be found in these refs[10,11,35] and are summarized below. EMG was obtained from either the nuchal muscles or from correlated high-frequency (300–600 Hz) signals from brain electrodes[10,49]. All experimental procedures were in accordance with the National Institutes of Health guidelines and approved by the University of Wisconsin-Milwaukee, New York University, and Weill Cornell Medical College Institutional Animal Care and Use Committees. Numbers of analyzed cells and states/transitions for each dataset are summarized in Table 1. To estimate firing rates reliably, only NREM > 150 s (accounting for 462/534 NREM epochs in hippocampal sessions and 232/282 NREM epochs in neocortical sessions) and REM > 100 s (277/371 REM epochs in hippocampal sessions and 123/252 REM epochs in neocortical sessions) were used for all analyses.

**Time normalized mean firing rates.** In the series of analyses of sleep sequences (e.g. Fig. 1B,E and similar) NREM and REM epochs were divided into 30 bins and 10 bins, respectively, since NREM epochs are generally longer. Additionally, cells were sorted into quintiles within each epoch and firing rates of cells in each quintile were calculated in each bin. Importantly, sorting was based on their mean firing rates over the entirety of the windows of interests depicted in each panel, to avoid RTM effects which are particularly evident when tracking ranked groups of units such as quintiles. While ranking was based on the entire epoch in these analyses, to allow for comparisons across quintiles, firing rates were normalized by the mean firing rate in the last one-third of the first state.

**Change index and deflection index.**    For a second set of analyses, change index (*CI*) for a quintile was defined as $(\overline{FR_i} - \overline{FR_j})/(\overline{FR_i} + \overline{FR_j})$, where $FR_i$ and $FR_j$ are mean firing rates of a neuron over time periods $i$ and $j$ ($i < j$), respectively, and $\overline{FR_x}$ is the mean of the mean $FR_x$ over the neurons in the quintile. Neurons were first separated into quintiles based on $FR_i$ within each epoch, and quintile *CI* was then calculated across a given pair of epochs. If more than 20% of cells did not fire in epoch $i$ or $j$, that sequence was excluded from the analyses since *CI* for the lowest quintile cannot be properly calculated in such a case. Note that this analysis still allows for changes in quintile membership between $i$ and $j$. Because neuronal firing rates are log-normally distributed, the difference in logarithm of firing rates, $\Delta log(FR)$, had been previously used to assess firing rate changes[10]. Although *CI* and $\Delta log(FR)$ generally behave similarly, $\Delta log(FR)$ becomes singular when either $FR_i$ or $FR_j$ approach or equal zero. Therefore, in these analyses we opted to use *CI*.

Our null hypothesis was that changes across states are not different than changes within states, allowing for RTM. To evaluate the corresponding null distribution for this analysis, we generated 2000 shuffled surrogates by random flipping of $FR_i$ and $FR_k$ for each cell, where $k$ is a control period of the same state as $i$. For analyses involving sleep, these control periods were taken from the corresponding periods (e.g. first/last one-third) in adjacent epochs of the same state (NREM or REM). Note that by chance these surrogate *CI*s therefore involve changes either forward or backward in time and always either ending or originating in epoch $i$. For transitions involving WAKE, control periods were randomly selected from 1-min periods of the same wake epoch (since wake periods separated by sleep display significantly different firing rates[11,12]). Shuffled mean and 95% confidence intervals of *CI* were obtained from this surrogate data. The deflection index (*DI*) was defined as difference of *CI* from the surrogate mean.

**Detection of OFF states, microarousals, and LOW states.**    We labeled periods with no spikes from any recorded units for >75 ms as OFF states[12,61] in both hippocampal and frontal cortical recordings. Following our previously published methods, transient (>0.1 s and <40 s) increase of EMG signal (>mean + 0.5 SD for hippocampal sessions and >local minima of EMG power for neocortical sessions) within NREM were marked as microarousals (MAs)[10,35]. LOW states were detected as periods with a transient drop of LFP power in the 0.625 to 50 Hz band, calculated in 0.1-s step sliding 1-s windows[35]. The threshold for each session were determined based on histogram of the power within NREM epochs (see ref.[35] for additional details).

**Simulations.**    To better understand the behavior of *CI* and *DI* we generated three random datasets involving noise combined with no-change, additive firing rate increase, and multiplicative firing rate increase. Each dataset has 5000 cells and 3 epochs, corresponding to epochs $i$, $j$, and $k$. To mimic the variability of real data, first we set a baseline firing rate for each cell based on a log-normal distribution obtained from hippocampal pyramidal cells during NREM (mean = 0.59 Hz, std = 0.84 Hz) and then added random ("multiplicative") noise proportional to each cell's firing rate in each epoch (std = 0.35 Hz). For the no-change simulation, each cell kept the same baseline firing rates across epochs with only random noise producing fluctuation across epochs. For additive and multiplicative increase simulations, baseline firing rates in epoch $j$ were increased (by addition of 0.05 Hz or multiplication by 1.1 for additive and multiplicative increases, respectively).

**Additional statistical analyses.**    In this work we analyzed previously obtained data and no additional experiments were performed. Diversity of firing rates was evaluated by coefficient of variance (CV) and significance of difference was tested with Wilcoxon rank sum test. P-values of *DI*s were calculated relative to shuffled surrogates. Differences in *DI* and firing rate changes among quintiles were tested with one-way ANOVA. Firing rate distributions were compared by a Kolmogorov-Smirnov test. All analyses were performed with custom-written scripts running on MATLAB with statistics and machine learning tool boxes. Code is available upon request.

## Data Availability

Frontal cortical data used in this study is available on CRCNS.org[62]. Hippocampal data will be made available upon reasonable request.

## References

1. Stuart, G. J. & Spruston, N. Dendritic integration: 60 years of progress. *Nat Neurosci* **18**, 1713–1721 (2015).
2. Lim, S. *et al.* Inferring learning rules from distributions of firing rates in cortical neurons. *Nat Neurosci* **18**, 1804–1810 (2015).
3. Roxin, A., Brunel, N., Hansel, D., Mongillo, G. & van Vreeswijk, C. On the distribution of firing rates in networks of cortical neurons. *J Neurosci* **31**, 16217–16226 (2011).
4. Koulakov, A. A., Hromadka, T. & Zador, A. M. Correlated connectivity and the distribution of firing rates in the neocortex. *J Neurosci* **29**, 3685–3694 (2009).
5. Nigam, S. *et al.* Rich-Club Organization in Effective Connectivity among Cortical Neurons. *J Neurosci* **36**, 670–684 (2016).
6. Yassin, L. *et al.* An embedded subnetwork of highly active neurons in the neocortex. *Neuron* **68**, 1043–1050 (2010).
7. Cheng, S. & Frank, L. M. New experiences enhance coordinated neural activity in the hippocampus. *Neuron* **57**, 303–313 (2008).
8. Lee, D., Lin, B. J. & Lee, A. K. Hippocampal place fields emerge upon single-cell manipulation of excitability during behavior. *Science* **337**, 849–853 (2012).
9. Hengen, K. B., Lambo, M. E., Van Hooser, S. D., Katz, D. B. & Turrigiano, G. G. Firing rate homeostasis in visual cortex of freely behaving rodents. *Neuron* **80**, 335–342 (2013).
10. Watson, B. O., Levenstein, D., Greene, J. P., Gelinas, J. N. & Buzsáki, G. Network Homeostasis and State Dynamics of Neocortical Sleep. *Neuron* **90**, 839–852 (2016).
11. Miyawaki, H. & Diba, K. Regulation of Hippocampal Firing by Network Oscillations during Sleep. *Curr Biol* **26**, 893–902 (2016).
12. Vyazovskiy, V. V. *et al.* Cortical firing and sleep homeostasis. *Neuron* **63**, 865–878 (2009).
13. Turrigiano, G. Too many cooks? Intrinsic and synaptic homeostatic mechanisms in cortical circuit refinement. *Annu Rev Neurosci* **34**, 89–103 (2011).

14. Marder, E. & Goaillard, J. M. Variability, compensation and homeostasis in neuron and network function. *Nat Rev Neurosci* **7**, 563–574 (2006).
15. Hengen, K. B., Torrado Pacheco, A., McGregor, J. N., Van Hooser, S. D. & Turrigiano, G. G. Neuronal Firing Rate Homeostasis Is Inhibited by Sleep and Promoted by Wake. *Cell* **165**, 180–191 (2016).
16. Grosmark, A. D., Mizuseki, K., Pastalkova, E., Diba, K. & Buzsaki, G. REM sleep reorganizes hippocampal excitability. *Neuron* **75**, 1001–1007 (2012).
17. Hobson, J. A. & Pace-Schott, E. F. The cognitive neuroscience of sleep: neuronal systems, consciousness and learning. *Nat Rev Neurosci* **3**, 679–693 (2002).
18. Brown, R. E., Basheer, R., McKenna, J. T., Strecker, R. E. & McCarley, R. W. Control of sleep and wakefulness. *Physiol Rev* **92**, 1087–1187 (2012).
19. Weber, F. & Dan, Y. Circuit-based interrogation of sleep control. *Nature* **538**, 51–59 (2016).
20. Saper, C. B., Fuller, P. M., Pedersen, N. P., Lu, J. & Scammell, T. E. Sleep state switching. *Neuron* **68**, 1023–1042 (2010).
21. Tononi, G. & Cirelli, C. Sleep and the price of plasticity: from synaptic and cellular homeostasis to memory consolidation and integration. *Neuron* **81**, 12–34 (2014).
22. Gulati, T., Guo, L., Ramanathan, D. S., Bodepudi, A. & Ganguly, K. Neural reactivations during sleep determine network credit assignment. *Nat Neurosci* **20**, 1277–1284 (2017).
23. Bartram, J. *et al.* Cortical Up states induce the selective weakening of subthreshold synaptic inputs. *Nat Commun* **8**, 665 (2017).
24. Grosmark, A. D. & Buzsaki, G. Diversity in neural firing dynamics supports both rigid and learned hippocampal sequences. *Science* **351**, 1440–1443 (2016).
25. Margolis, D. J. *et al.* Reorganization of cortical population activity imaged throughout long-term sensory deprivation. *Nat Neurosci* **15**, 1539–1546 (2012).
26. Xie, X., Hahnloser, R. H. R. & Seung, H. S. Selectively Grouping Neurons in Recurrent Networks of Lateral Inhibition. *Neural Comput* **14**, 2627–2646 (2002).
27. McCarley, R. W. & Hobson, J. A. Single neuron activity in cat gigantocellular tegmental field: selectivity of discharge in desynchronized sleep. *Science* **174**, 1250–1252 (1971).
28. Evarts, E. V. Temporal Patterns of Discharge of Pyramidal Tract Neurons during Sleep and Waking in the Monkey. *J Neurophysiol* **27**, 152–171 (1964).
29. Niethard, N. *et al.* Sleep-Stage-Specific Regulation of Cortical Excitation and Inhibition. *Curr Biol* **26**, 2739–2749 (2016).
30. Renouard, L. *et al.* The supramammillary nucleus and the claustrum activate the cortex during REM sleep. *Sci Adv* **1**, e1400177 (2015).
31. Tsodyks, M. V., Skaggs, W. E., Sejnowski, T. J. & McNaughton, B. L. Population dynamics and theta rhythm phase precession of hippocampal place cell firing: a spiking neuron model. *Hippocampus* **6**, 271–280 (1996).
32. Hahn, T. T., Sakmann, B. & Mehta, M. R. Phase-locking of hippocampal interneurons' membrane potential to neocortical up-down states. *Nat Neurosci* **9**, 1359–1361 (2006).
33. Basu, J. *et al.* Gating of hippocampal activity, plasticity, and memory by entorhinal cortex long-range inhibition. *Science* **351**, aaa5694 (2016).
34. Dehghani, N. *et al.* Dynamic Balance of Excitation and Inhibition in Human and Monkey Neocortex. *Sci Rep* **6**, 23176 (2016).
35. Miyawaki, H., Billeh, Y.N. & Diba, K. Low Activity Microstates During Sleep. *Sleep* **40** (2017).
36. Watson, B. O. Cognitive and Physiologic Impacts of the Infraslow Oscillation. *Front Syst Neurosci* **12**, 44 (2018).
37. Steriade, M., Nunez, A. & Amzica, F. A novel slow (<1 Hz) oscillation of neocortical neurons *in vivo*: depolarizing and hyperpolarizing components. *J Neurosci* **13**, 3252–3265 (1993).
38. Destexhe, A., Hughes, S. W., Rudolph, M. & Crunelli, V. Are corticothalamic 'up' states fragments of wakefulness? *Trends Neurosci* **30**, 334–342 (2007).
39. Jarosiewicz, B. & Skaggs, W. E. Hippocampal place cells are not controlled by visual input during the small irregular activity state in the rat. *J Neurosci* **24**, 5070–5077 (2004).
40. Nadim, F. & Bucher, D. Neuromodulation of neurons and synapses. *Curr Opin Neurobiol* **29**, 48–56 (2014).
41. Graves, A. R. *et al.* Hippocampal pyramidal neurons comprise two distinct cell types that are countermodulated by metabotropic receptors. *Neuron* **76**, 776–789 (2012).
42. Steriade, M., Timofeev, I. & Grenier, F. Natural waking and sleep states: a view from inside neocortical neurons. *J Neurophysiol* **85**, 1969–1985 (2001).
43. Timofeev, I., Grenier, F. & Steriade, M. Disfacilitation and active inhibition in the neocortex during the natural sleep-wake cycle: an intracellular study. *Proc Natl Acad Sci USA* **98**, 1924–1929 (2001).
44. Stringer, C. *et al.* Inhibitory control of shared variability in cortical networks. *eLife*, https://doi.org/10.7554/eLife.19695 (2016).
45. Kuchibhotla, K.V. *et al.* Parallel processing by cortical inhibition enables context-dependent behavior. *Nat Neurosci* (2016).
46. Yuille, A.L. & Geiger, D. Winner-take-all mechanisms. In *Handbook of Brain Theory and Neural Networks* (ed. M.A. Arbib) 1–1056 (Mit Press, 1995).
47. Lee, D. K., Itti, L., Koch, C. & Braun, J. Attention activates winner-take-all competition among visual filters. *Nat Neurosci* **2**, 375–381 (1999).
48. Rutishauser, U., Douglas, R. J. & Slotine, J. J. Collective stability of networks of winner-take-all circuits. *Neural Comput* **23**, 735–773 (2011).
49. Schomburg, E. W. *et al.* Theta phase segregation of input-specific gamma patterns in entorhinal-hippocampal networks. *Neuron* **84**, 470–485 (2014).
50. Mizuseki, K., Diba, K., Pastalkova, E. & Buzsaki, G. Hippocampal CA1 pyramidal cells form functionally distinct sublayers. *Nat Neurosci* **14**, 1174–1181 (2011).
51. Hasselmo, M. E. The role of acetylcholine in learning and memory. *Curr Opin Neurobiol* **16**, 710–715 (2006).
52. Gottesmann, C. Detection of seven sleep-waking stages in the rat. *Neurosci Biobehav Rev* **16**, 31–38 (1992).
53. Cirelli, C. Sleep, synaptic homeostasis and neuronal firing rates. *Curr Opin Neurobiol* **44**, 72–79 (2017).
54. Olcese, U., Esser, S. K. & Tononi, G. Sleep and synaptic renormalization: a computational study. *J Neurophysiol* **104**, 3476–3493 (2010).
55. de Vivo, L. *et al.* Ultrastructural evidence for synaptic scaling across the wake/sleep cycle. *Science* **355**, 507–510 (2017).
56. Danielson, N. B. *et al.* Sublayer-Specific Coding Dynamics during Spatial Navigation and Learning in Hippocampal Area CA1. *Neuron* **91**, 652–665 (2016).
57. Molyneaux, B. J., Arlotta, P., Menezes, J. R. & Macklis, J. D. Neuronal subtype specification in the cerebral cortex. *Nat Rev Neurosci* **8**, 427–437 (2007).
58. Isomura, Y. *et al.* Integration and segregation of activity in entorhinal-hippocampal subregions by neocortical slow oscillations. *Neuron* **52**, 871–882 (2006).
59. Csicsvari, J., Hirase, H., Czurko, A. & Buzsaki, G. Reliability and state dependence of pyramidal cell-interneuron synapses in the hippocampus: an ensemble approach in the behaving rat. *Neuron* **21**, 179–189 (1998).
60. Bartho, P. *et al.* Characterization of neocortical principal cells and interneurons by network interactions and extracellular features. *J Neurophysiol* **92**, 600–608 (2004).

61. Ji, D. & Wilson, M. A. Coordinated memory replay in the visual cortex and hippocampus during sleep. *Nat Neurosci* **10**, 100–107 (2007).
62. Watson, B. O., Levenstein, D., Greene, J. P., Gelinas, J. N. & G. B. Multi-unit spiking activity recorded from rat frontal cortex (brain regions mPFC, OFC, ACC, and M2) during wake-sleep episode wherein at least 7 minutes of wake are followed by 20 minutes of sleep. (CRCNS.org, 2016).

## Author Contributions

All authors designed research. H.M. and B.O.W. performed research. H.M. and K.D. analyzed data. H.M. and K.D. wrote the paper. All authors edited the paper.

## Additional Information

**Supplementary information** accompanies this paper at https://doi.org/10.1038/s41598-018-36710-8.

**Competing Interests:** The authors declare no competing interests.

**Publisher's note:** Springer Nature remains neutral with regard to jurisdictional claims in published maps and institutional affiliations.